

AD-A252 925



2

NAVAL POSTGRADUATE SCHOOL

Monterey, California



S DTIC
ELECTE
JUL 16 1992 **A** **D** THESIS

RADIATION STRESS SPECTRAL TRANSFORMATION
ACROSS THE SURF ZONE

by

Thomas D. McGowan

March 1992

Thesis Advisor:

Edward B. Thornton

Approved for public release; distribution is unlimited



92-18868

00 0 11 000

Unclassified

SECURITY CLASSIFICATION OF THIS PAGE

REPORT DOCUMENTATION PAGE

Form Approved
OMB No. 0704-0188

1a. REPORT SECURITY CLASSIFICATION UNCLASSIFIED			1b. RESTRICTIVE MARKINGS		
2a. SECURITY CLASSIFICATION AUTHORITY			3. DISTRIBUTION/AVAILABILITY OF REPORT Approved for public release; distribution is unlimited		
2b. DECLASSIFICATION/DOWNGRADING SCHEDULE					
4. PERFORMING ORGANIZATION REPORT NUMBER(S)			5. MONITORING ORGANIZATION REPORT NUMBER(S)		
6a. NAME OF PERFORMING ORGANIZATION Naval Postgraduate School		6b. OFFICE SYMBOL OC	7a. NAME OF MONITORING ORGANIZATION		
6c. ADDRESS (City, State, and ZIP Code) Monterey, CA 93943-5000			7b. ADDRESS (City, State, and ZIP Code)		
8a. NAME OF FUNDING/SPONSORING ORGANIZATION		8b. OFFICE SYMBOL	9. PROCUREMENT INSTRUMENT IDENTIFICATION NUMBER		
8c. ADDRESS (City, State, and ZIP Code)			10. SOURCE OF FUNDING NUMBERS		
			PROGRAM ELEMENT NO.	PROJECT NO.	TASK NO.
			WORK UNIT ACCESSION NO.		
11. TITLE (Including Security Classification) Radiation Stress Spectral Transformation Across the Surf Zone					
12. PERSONAL AUTHOR(S) McGowan, Thomas D.					
13. TYPE OF REPORT Master's thesis		13b. TIME COVERED FROM TO		14. DATE OF REPORT (Year, Month, Day) 1992, MARCH	
				15. Page Count 39	
16. SUPPLEMENTAL NOTATION The views expressed in this thesis are those of the author and do not reflect the official policy or position of the Department of Defense or the U.S. Government.					
17. COSATI CODES			18. SUBJECT TERMS (Continue on reverse if necessary and identify by block number)		
FIELD	GROUP	SUB-GROUP			
19. ABSTRACT (Continue on reverse if necessary and identify by block number)					
<p>Shoaling and decay of bi-modal spectra (two distinct frequency peaks and directions) were measured at Santa Barbara Beach, California. Spectral analysis shows that the wave train associated with the lower frequency peak dominates in the surf zone with the high frequency component decaying faster than low frequency component. Mean wave directions were measured for both wave trains with current meters located outside and throughout the surf zone. Errors associated with meter is-alignment were minimized by numerically rotating the measured mean wave direction of the low frequency wave component to correspond with the predicted refracted direction based on Snell's Law over the near planar beach. Meter re-alignments were then verified by comparing the measured and predicted directions of the high frequency component, yielding an average error of order one degree. The ability to remove rotational errors from in-situ data thereby allows for accurate measurements of the radiation stress transformation across the surf zone.</p>					
20. DISTRIBUTION/AVAILABILITY OF ABSTRACT <input checked="" type="checkbox"/> UNCLASSIFIED/UNLIMITED <input type="checkbox"/> SAME AS RPT. <input type="checkbox"/> DTIC			1a. REPORT SECURITY CLASSIFICATION		
22a. NAME OF RESPONSIBLE INDIVIDUAL Edward B. Thornton			22b. TELEPHONE (include Area Code) (408)646-2847		22c. OFFICE SYMBOL OC/Tm

Approved for public release; distribution is unlimited

Radiation Stress Spectral Transformation Across the Surf Zone

by

Thomas D. McGowan
Lieutenant, United States Navy
BS, University of New Hampshire, 1983

Submitted in partial fulfillment
of the requirements for the degree

MASTER OF SCIENCE IN PHYSICAL OCEANOGRAPHY

from the

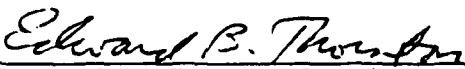
NAVAL POSTGRADUATE SCHOOL
Monterey California


March 1992

Author:


Thomas D. McGowan

Approved by:


Edward B. Thornton, Thesis Advisor


Kim, Chang-Shik, Second Reader



Curtis A. Collins, Chairman,
Department of Oceanography

TABLE OF CONTENTS

I.	INTRODUCTION	1
II.	EXPERIMENT	6
III.	RADIATION STRESS SPECTRAL CALCULATIONS	9
IV.	DISCUSSION	15
V.	CONCLUSIONS	20
	LIST OF REFERENCES	32
	INITIAL DISTRIBUTION LIST	34

Accession For	
NTIS CRA&I	<input checked="" type="checkbox"/>
DTIC TAB	<input type="checkbox"/>
Unannounced	<input type="checkbox"/>
Justification	
By	
Distribution /	
Availability Codes	
Dist	Avail and/or Special
A-1	

ABSTRACT

Shoaling and decay of bi-modal spectra (two distinct frequency peaks and directions) were measured at Santa Barbara Beach, California. Spectral analysis shows that the wave train associated with the lower frequency peak dominates in the surf zone with the high frequency component decaying faster than the low frequency component. Mean wave directions were measured for both wave trains with current meters located outside and throughout the surf zone. Errors associated with meter mis-alignment were minimized by numerically rotating the measured mean wave direction of the low frequency wave component to correspond with the predicted refracted direction based on Snell's Law over the near planar beach. Meter re-alignments were then verified by comparing the measured and predicted directions of the high frequency component, yielding an average error of order one degree. The ability to remove rotational errors from in-situ data thereby allows for accurate measurements of the radiation stress transformation across the surf zone.

I. INTRODUCTION

In analyzing surf zone longshore currents, the focus on model development has been on uni-directional monochromatic waves or random wave fields that are narrowbanded in frequency and direction. The models have yet to be extended to broadbanded (either in frequency or direction) wave fields because of the difficulty of parameterizing the breaking of such a wave field or the interactions between energetic frequency bands. Modern theories (Bowen, 1969; Thornton, 1970; Longuet-Higgins, 1970) have theoretically established that the driving force for longshore currents is the cross-shore gradient of radiation stress, $S_{xy}(f)$, which describes the onshore flux of alongshore wave-induced momentum, integrated over the depth, h , and averaged over time, t ,

$$S_{xy}(f) = \overline{\int_{-h}^0 u(z,f,t) v(z,f,t) dz} \quad (1)$$

where u,v are the horizontal x,y velocity components, z is the vertical elevation, and f is the frequency.

The radiation stress can be calculated from the co-spectrum, $C_{uv}(f)$, of the u and v velocity components measured at depth, z , and transformed using a linear theory transfer function, $H_1(f)$,

$$S_{xy}(f) = |H_1(f)|^2 C_{xy}(f) \quad (2)$$

where

$$|H_1(f)|^2 = \frac{\rho}{2k} \frac{1}{\cosh^2 k(h+z)} \left[\frac{\sinh 2kh}{2} + kh \right]$$

and ρ is the density and k is the wave number. An equivalent form for $S_{xy}(f)$ expressed in terms of linear theory is:

$$S_{xy}(f) = E(f) c_g(f) \cos \alpha(f) \frac{\sin \alpha(f)}{c(f)} \quad (3)$$

where $E(f)$ is the energy, $c_g(f)$ and $c(f)$ the group and phase speed, and $\alpha(f)$, the angle of wave incidence from normal. Along plane parallel depth contours before dissipation by wave breaking, $S_{xy}(f)$ is conserved during the shoaling process. When waves break, there is a decrease in the radiation stress associated with the reduction in wave energy.

For a broadband wave field (both in frequency and direction) the total radiation stress, S_{xy}^T , is the sum of the individual wave components

$$S_{xy}^T = \int_{f_1}^{f_2} S_{xy}(f) df. \quad (4)$$

Guza et al (1986) concluded that the total radiation stress, S_{xy}^T , and not the structure of $S_{xy}(f)$ is of primary importance in determining the magnitude of the resulting longshore currents.

Direct measurements of the radiation stress and radiation stress gradient are difficult and have not been accurately made for use in testing of longshore current models. Small incident wave angles make the gradient measurements highly sensitive to current meter orientation errors, and even with proper sensor orientation, the directional response of the sensors is not well known (Guza and Thornton, 1978). While the energy density and quadrature spectra are invariant with coordinate rotation, the co-spectrum, used to calculate radiation stress, is very sensitive to coordinate rotation or current meter misalignment. Guza and Thornton (1978) showed that the relative error in the radiation stress at a particular frequency can be approximated for small angle of wave incidence by,

$$Rel\ error = \frac{\Delta}{\alpha(f)} \quad (5)$$

where Δ is the angular error. Angular errors may be caused by lack of instrument directional resolution, installation misalignment, and in-situ rotation due to environmental conditions. Grosskopf et al. (1983) judged that the maximum combined error due to resolution of Marsh-McBirney electromagnetic current meters and meter orientation using a flux gate compass to be ± 5 degrees. This says, that

for an incident wave angle of 10 degrees and an error of ± 5 degrees in meter alignment, a 50 % relative error in radiation stress calculations would result.

A complete description of the radiation stress for a broad banded wave field requires specifying wave energy-density directional spectra. The interaction of even two wave components shoaling across the surf zone is complicated. Smith and Vincent (1992) studied the breaking and interactions of two irregular wave trains having two distinct frequency peaks in a laboratory wave flume (collinear in direction). They found that the wave train with the low frequency peak appears unaffected by the presence of the higher frequency wave train, but the high frequency wave train decays faster in the presence of the low frequency waves. This result was independent of both the relative distribution of energy between the two and the amount of separation between the frequency peaks. It should also be noted that although the spectral-based significant wave height of the dual system decayed similarly to a single wave system, if the surf zone wave heights measured in the two individual tests were superimposed the combined wave height was too large, suggesting significant nonlinear interactions in the breaking process. Therefore, radiation stress and resulting longshore current estimates using linear superposition of wave height would not be accurate.

The purpose of this paper is to demonstrate that current meters can be uniquely orientated based on wave refraction of a bi-modal directional wave spectra, allowing the radiation stress to be accurately calculated. Bi-modal data sets are chosen that contain waves from two opposing directions, one a locally generated high

frequency sea, the other, low frequency ocean swell. Mean wave spectral directions are calculated using current meters located outside and throughout the surf zone. These mean directions are compared with directions obtained by shoaling the low frequency swell shoreward over the near planar beach using Snell's Law. The difference between the measured mean wave direction and the direction calculated from shoaling with Snell's Law are used as a basis for meter re-alignment. A constraint on the magnitude of the radiation stress energy flux calculations is that they are conserved outside the surf zone and monotonically decay over the straight and parallel contours. Radiation stress calculations after re-alignment are in good agreement with theory.

In the following, the experiment and the incident wave field are discussed first. Next, the transformation of the bi-modal spectra across the surf zone are described in terms of the energy transformation, directional computations and meter re-orientation, and radiation stress transformation. Ramifications for broadbanded data are addressed in the discussion, followed by conclusions.

II. EXPERIMENT

Field measurements were obtained at Leadbetter Beach in Santa Barbara, California from 30 January - 23 February 1980. The experiment was part of the Nearshore Sediment Transport Study (NSTS). The overall objective of the study was to develop relations for the prediction of sediment transport by waves and currents in the nearshore environment (Gable, 1981). The field experiments were set up to measure, simultaneously, the details of both the velocity field within the surf zone and the sediment response to these velocities. By characterizing the wave and horizontal velocity fields in the surf zone, the forcing function for sediment transport could be analyzed and eventually modelled. The Leadbetter Beach site was chosen because it can be reasonably assumed in the near shore that the waves are homogeneous in the alongshore direction and that bottom contours are straight and parallel, simplifying the analysis. The bathymetry and locations of sensors used in the study are shown in Figure 1.

The shoreline at Leadbetter beach has an unusual east-west orientation along a predominantly north-south coast. Open ocean waves are limited to a narrow window of approach (240-258 degrees, Figure 2) because of the protection from Point Conception to the north and the Channel Islands to the south. The generally highly directional filtered ocean swell from the North Pacific approach the beach from

almost due west, resulting in large oblique angles relative to the surf zone bottom contours.

On February 6, the first of a three week series of storms began, which have been categorized as 1 in 25 to 1 in 40 year storms. Strong winds associated with these storms created a locally wind driven sea inside the Channel Islands from a range of directions, but waves came mainly from the south-east window (123-143 degrees). At the same time, a swell derived from the open ocean waves was also present, resulting in a bi-modal or broad banded wave spectrum. The data on 13 and 16 February are chosen for analysis, since they had the largest number of operational current meters in the cross-shore direction, and best depict bi-modal spectra.

As many as 24 electromagnetic current meters and 14 pressure sensors were simultaneously deployed. The electromagnetic current meters were Marsh-McBirney Model 512 with 4 cm diameter spherical probes. The instruments were most densely spaced in the surf zone. The transect of instruments starting in 4 meter depth is shown in Figure 3, drawn to scale, showing the near planar sloping beach and a typical deep ocean swell with a period of 14 seconds well resolved by the array of instruments. Instruments not shown in deeper water include a current meter at 7 meter depth (*C0d*) and a slope array (*SA*) composed of four pressure sensors at 9 meter depth (see Figure 1). The wave staffs shown were part of a moveable spider assembly, where up to four current meters could be deployed in cross-shore direction.

Data runs were at high tide with water levels between about 0 and +100 cm above mean sea water level (MSWL). Quality control over instrument orientation

was maintained by checking all surf zone current meters at low tide prior to high tide. Meter orientation at low tide (for exposed meters) was accomplished using a specially designed sighting bracket (Gable, 1981). Meters located in deeper water were orientated by divers using flux gate compasses. Throughout the experiment, especially during large wave conditions, *Macrocystis* kelp would break loose and find its way to the beach. This posed a serious problem due to entanglement of the kelp with the instrumentation, causing bending or twisting of the current meters. The kelp problem was partially solved by positioning people updrift of the instruments to intercept and manually remove and deposit the kelp on the beach. This procedure, though, was only partly successful. Further details of the experiment are given in Thornton and Guza (1986) and references therein.

III. RADIATION STRESS SPECTRAL CALCULATIONS

Eight hours of data were acquired at a sampling frequency of 2 Hz on both the 13th and 16th of February. Both days were non-stationary, with the most variation associated with the locally driven storm. On both days the storm increased in intensity, peaked, and then tapered off by the end of the day. The high frequency shifts were from 0.211 Hz to 0.113 Hz on the 13th and 0.203 Hz to 0.148 Hz on the 16th. Because of this non-stationary behavior, the records selected were limited in length to 64 minutes and chosen during times of least change. Each 64 minute run was broken into 30 subsets for spectral representation, yielding 60 degrees of freedom and a frequency resolution of 0.0078 Hz.

Linear theory transfer functions are used to calculate energy, energy flux, and radiation stress. Snell's Law is used to refract waves over the straight and parallel contours at Santa Barbara. The energy flux, $F(f)$ is calculated from the energy, $E(f)$, and the group speed, $c_g(f)$. The energy is calculated using the spectra of the u and v velocity components, $G_x(f)$ and $G_y(f)$, measured at depth z , and transformed using a linear theory transfer function $H_2(f)$.

$$F(f) = E(f) * c_g(f) \quad (6)$$

where

$$E(f) = |H_2(f)|^2 [G_x(f) + G_y(f)] \quad (7)$$

and

$$|H_2(f)|^2 = \frac{\rho \sinh(2kh)}{4k \cosh^2 k(h+z)}$$

where ρ is density, k wave number, h total depth of water, g gravity, and $c_g(f)$ is described by linear wave theory. The total energy flux, F , is found by integrating over the desired frequency band.

$$F = \int_{f_1}^{f_2} F(f) df \quad (8)$$

The energy flux spectra at 12 current meter locations on the 13th (*C - 0d, 01, 03, 07, 11, 13, 14, 15, 16, 17, 20, 21, 22*) and 11 current meter locations on the 16th, (*C - 0d, 01, 03, 04, 07, 11, 13, 15, 16, 20, 19, 18*) are shown in Figures 4a,b. The sea swell from the west window had a frequency peak centered about 0.063 Hz on the 13th and increased to 0.078 Hz on the 16th as the storm grew in intensity and moved northward. The locally generated sea from the east, had a frequency peak of 0.211 Hz on the 13th and a different storm cell on the 16th had a frequency peak of 0.203 Hz. The energy flux summed over the low frequency, high frequency, and, both wave components is also shown in Figures 4a,b with the integration limits noted in the captions. Linear theory predicts that the energy flux is conserved until wave breaking and then monotonically decreases shoreward. The analysis for both days support this, suggesting that wave breaking commences in approximately 2.0 meters of water on

the 13th and 2.4 meters of water on the 16th. The wave climate on the 13th was characterized by moderate waves (significant wave height, $H_s = 0.9$ m), with moderate to high waves ($H_s = 1.2$ m) on the 16th. A 6.5 % gain increase was applied to current meter *C01*, as suggested by Guza et al. (1986), because energy flux estimates from a pressure sensor co-located there were in better agreement with *C0d* and *C03*.

As in laboratory experiments conducted by Smith and Vincent (1992), the spectra show that the high frequency component dissipates faster than the low frequency component. On the 13th, 85 % of the total energy flux in deeper water (6.8 m) is at the high frequency component, decaying to 50% at a depth of 1.0 meters, with no noticeable energy flux contribution shoreward of this depth (Figure 4a). On the 16th, the energy flux is equally distributed for both high and low frequency components starting in 6.8 meters of water, with the high frequency component becoming negligible by a depth of 1.0 meters (Figure 4b).

Radiation stress spectral calculations in the past have been suspect due to the inability to accurately resolve meter orientation. To remove these errors, the mean wave direction is calculated using the co-spectrum, $C_{uv}(f)$, and energy spectra, $G_x(f)$ and $G_y(f)$, of the u and v velocity components, (Long 1980)

$$\alpha(f) = \frac{2C_{uv}(f)}{G_x(f) - G_y(f)} \quad (9)$$

Since most instrument locations consisted of only a current meter, only the mean wave direction is calculated which can be obtained from a single current meter, instead of the full directional spectra which requires a collocated pressure sensor.

The mean wave direction is determined at the peak frequency of both energetic wave components at each current meter location (solid lines in upper panel of Figures 5a,b). The coordinate system chosen for analysis was zero degrees perpendicular to the beach, +90.0 degrees to the east, and -90.0 degrees to the west. Bias in the mean wave direction at the peak frequency was checked by comparing values about adjacent frequency bins, which showed comparable values. Also computed at each location is the predicted wave direction derived from shoaling the mean wave direction at the deep water current meter, *C0d*, shoreward using Snell's Law (dashed lines in upper panel of Figures 5a,b). The starting mean wave directions at *C0d* were verified against the directions derived from refracting the incident wave field directions measured at the slope array located in 9 m of water; this resulted in a -1 degree rotation of *C0d* (to the west). Large variations are noted between measured and predicted wave angles (upper panels of Figure 5a,b).

The current meters were then numerically rotated based on matching the measured mean wave direction for the low frequency component with its predicted wave direction derived from Snell's Law. The low frequency component is chosen as the basis of comparisons since it had energy present at all current meter locations, while the energy associated with the high frequency component dissipated completely at the most shoreward locations (Figure 4a,b). The differences between the

measured and predicted directions following meter re-alignment are shown in the lower panels of Figures 5a,b. The low frequency component directions, used as the basis of rotation, are exact and the corrected high frequency component directions show only small deviations. This not only indicates that the technique is viable, but shows Snell's Law is applicable throughout the surf zone, at least for these moderate wave conditions. Neglecting the three most shoreward meter locations for each day, where the high frequency wave energy has dissipated and the mean angle calculation (equation 9) is no longer accurate, the maximum error between measured and predicted wave directions following meter re-alignment is 3 degrees for the both the 13th and 16th, while the average error is 1.0 degrees for the 13th and 1.5 degrees for the 16th, both within the accuracy and resolution of the Marsh-McBirney current meters.

Radiation stress spectra, $S_{xy}(f)$, (equation 2), and the total radiation stress, S_{xy}^T , (equation 4), were calculated before and after meter re-orientation. Radiation stress spectral calculations prior to meter re-alignment (Figures 6a,7a), clearly show the need to resolve meter alignment. In several cases, the spectral plots show little correlation between adjacent meters and the total radiation stress deviates greatly from that predicted by theory. On the 16th, current meters C03 and C07 both misrepresent the radiation stress associated with each energetic wave, and current meter C15 shows the radiation stress for the low frequency component coming from the opposite quadrant (Figure 7a). Meter re-alignments for C03, C07, and C15 were -7,

+2, and +12 degrees respectively on the 16th. Following meter re-alignment (Figures 6b,7b) the total radiation stress is conserved outside the breaker zone and then decreases monotonically in agreement with the constraints of linear theory.

IV. DISCUSSION

To date, most research has been devoted towards narrow banded wave spectra. Of the 20 days of data acquired at Leadbetter Beach, only five days, with a narrow banded deep ocean swell present, have been extensively analyzed. Guza et al. (1986) investigated selected data over the entire period of the experiment for their radiation stress calculations, but limited the analysis to the two deep water current meters, *C0d* and *C0l*. Radiation stress estimates from current meters further inshore were judged too noisy and inconsistent with the estimates obtained from *C0d* and *C0l*. Radiation stress measurements prior to meter re-orientation (Figure 6a,7a) are indeed inconsistent with expected measurements, but once properly oriented, provide for a detailed examination of the cross-shore variation (Figure 7a,b).

Existing longshore current models are applicable for narrowbanded (in frequency and direction) spectra. They do not rely on direct measurements of the radiation stress, but use measured wave heights which are invariant to meter orientation. The longshore current is typically calculated from the measured wave heights and directional information at the peak frequency angle measured outside the breaker line and refracted shoreward.

Guza et al. (1986) noted that both the magnitude and the cross-shore variation of surf zone longshore currents appear insensitive to the structure of the spectral radiation stress, $S_{xy}(f)$, suppressing strong shear currents which would be suggested

by a bi-quadrant $S_{xy}(f)$ spectra. The nature of the wave climate on the 16th would suggest the possibility of shear currents, since both waves are of equal energy and of similar incident angles from opposite quadrants, but the total radiation stress, S_{xy}^T , does not show a significant reversal in sign (Figure 7b). As the radiation stress spectra transforms across the surf zone, the high frequency component decays faster than the low frequency component. Had the energy or the incident angle of the low frequency component been greater, the possibility of shear currents would seem likely. Smith and Vincent (1992) showed (in a wave flume) that the low frequency component appears unaffected by the presence of the high frequency component, regardless of the energy content in either component. Though laboratory results are not always indicative of the field results, the similar behavior of the energy flux transformation (Figure 4a,b) and radiation stress transformation (Figure 7a,b) presented here appears evident.

The radiation stress term is composed of both energy flux and directional information (equation 3). Even though there was substantial low frequency energy on the 13th, the longshore currents are driven mainly by the high frequency component of the radiation stress which had an initial incident angle of +30 degrees, while the low frequency component is almost zero due to the nearly normal initial wave incidence of -3 degrees (Figure 5a). The longshore currents on the 13th were of the order 1.0 m/s.

The total energy flux associated with the high frequency component on the 16th is nearly identical to that of the 13th (Figure 4a,b). However, opposing it on this day was equal energy from the low frequency component from the opposite quadrant, with a slightly smaller incident angle of, -17 degrees versus +23 degrees for the high frequency component. The total energy flux associated with the 16th is nearly double that of the 13th, but due to the opposing quadrants of approach of each wave component, the total radiation stress on the 16th is half of that on the 13th resulting in a smaller longshore current, of about 0.5 m/s.

Nearly identical radiation stress calculations can be obtained as those that were measured by linearly refracting the mean wave directional spectrum in deep water (*C0d*) and using the measured energy flux spectra in applying equation (3) to calculate $S_{xy}(f)$ at each current meter location (Figure 8a,b). The total radiation stress calculated in this manner appears more reasonable and is more consistent with linear theory inside the surf zone. Some of the inconsistencies in the measured radiation stress spectra inside the surf zone may be due to the fact that some of the current meters on the 16th were found to be bent, in some cases up to 45 degrees, resulting in errors which could account for the differences of the two techniques. Linear theory predicts that the celerity (wave phase speed) used in Snell's Law of refraction is frequency dispersive and decreases with increasing frequency. Thornton and Guza (1982) found that the measured celerity spectra are nondispersive with frequency as the waves approach and transect the surf zone indicating the importance of nonlinearities. The measured celerity at the peak frequencies was within +20 %

and -10 % of linear theory, with the percent difference generally increasing with the ratio of wave height to depth, indicating weak amplitude dispersion in shallow water. For the moderate wave conditions presented here, linear theory appears applicable, but errors can be introduced for larger waves due to nonlinearities.

Smith and Vincent (1992) have shown that linear superposition of wave heights for co-linear, bi-modal spectra over-predict the measured wave height and do not account for the dissipation of the high frequency component over that of the low frequency component. Linear theory does not account for the non-linearities of the wave breaking process or the complex interactions between wave components in a broadbanded wave field.

In an attempt to describe the shape of the wave spectrum during breaking, a similarity hypothesis is invoked (see for example Phillips, 1958; Thornton, 1977; Kitaigorodski et al, 1979; Bouws et al, 1985). Similarity assumes that during the breaking process a saturation in the high frequency region of the spectrum exists as energy is nonlinearly transferred down the spectrum. It is assumed that the excess energy of the high frequency wavelets is dissipated by breaking due to a kinematic instability in which the velocity of the wavelets exceed the phase speed. The relevant spectral parameters are then the phase speed and frequency. Dimensional analysis suggests that the energy flux in deepwater decays as f^{-6} , transitioning to a shallow water form of f^{-3} . Both the deep water and shallow water forms were applied to the energy flux spectra of the 13th and 16th (Figure 9a,b) by multiplying the energy flux by f^N and plotting the results on a logarithmic scale. For the f^N power law to hold

over a range of frequencies, the measured energy flux spectrum should be horizontal. The data is best represented by the shallow water form for the high frequency component with no evidence that either form would model the low frequency component. In very shallow depths, at the breaker line shoreward, the observed spectra tend to be less than the proposed f^{-3} limit (current meters *C19* and *C20*). Similar results were found on the 13th (figure 10a).

The complex interactions of a single wave train, during the shoaling and breaking process, have yet to be explained and modeled with satisfactory results, and the research towards understanding the dynamics of multiple wave trains is in the developmental stages. By analyzing a bi-modal spectra, both in the laboratory and the field, these interactions have been noted. The radiation stress for a bi-modal spectra suggests that given the proper wave conditions, shears in the longshore current are possible and only seen through direct measurements of the radiation stress across the surf zone. What has been provided is a technique that allows for accurate measurements of the radiation stress and a data set which can be used for testing broadbanded longshore current models.

V. CONCLUSIONS

The incident wave climate is rarely narrowbanded. Thompson (1980) concluded that the incident wave spectra are composed of two or more distinct wave trains, well separated in the frequency domain 65 % of the time. Thompson's statistics were from representative sites on the Atlantic, Pacific, and Gulf of Mexico coasts of the United States. The majority of the world's coastlines are open to waves from all directions with a protected coastline being an exception. Though the analysis of narrowbanded spectra is less complex, its actual applications are limited.

The locally generated storms that were experienced during the experiment conducted at Leadbetter Beach provided an excellent bi-modal wave field, separated both in frequency and direction. The protection of Leadbetter Beach afforded the opportunity of resolving the incident directions of each wave system. To resolve meter orientation, the incident wave fields must be separated in direction and these directions need to be accurately resolved.

The application of Snell's Law to a bi-modal spectra was verified for the moderate wave conditions present. Both wave components clearly showed that Snell's Law is valid outside and throughout the surf zone. The technique of meter re-orientation relies on an accurate measurement of the incident wave directions outside the surf zone and assumes that the errors introduced by applying linear shoaling theory are insignificant. Therefore, in future nearshore experiments it is

important to locate an accurate measurement of the wave directions, such as a linear array of pressure sensors, just outside the surf zone as a reference for resolving the orientation of current meters.

The primary instrument for nearshore experiments will continue to be the current meter since it can resolve both energy-density and direction. The technique presented allows the ability to correct for meter orientation errors and has shown that the directional resolution of the Marsh McBirney current meter is on the order of 1 degree, sufficient for accurate radiation stress measurements.

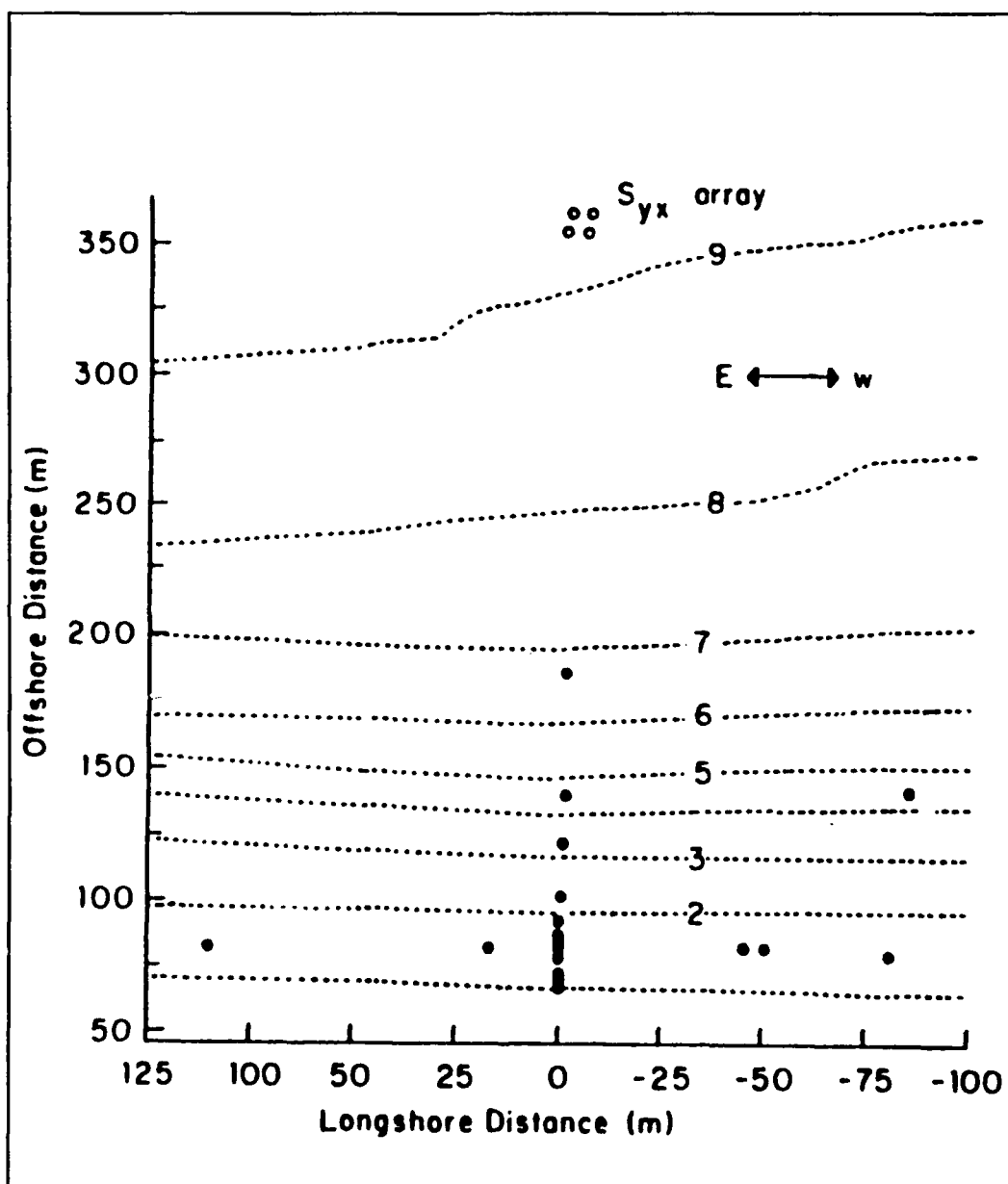


Figure 1 Nearshore bathymetry (contours are in meters) and sensor locations. Electromagnetic current meters are indicated by dots.

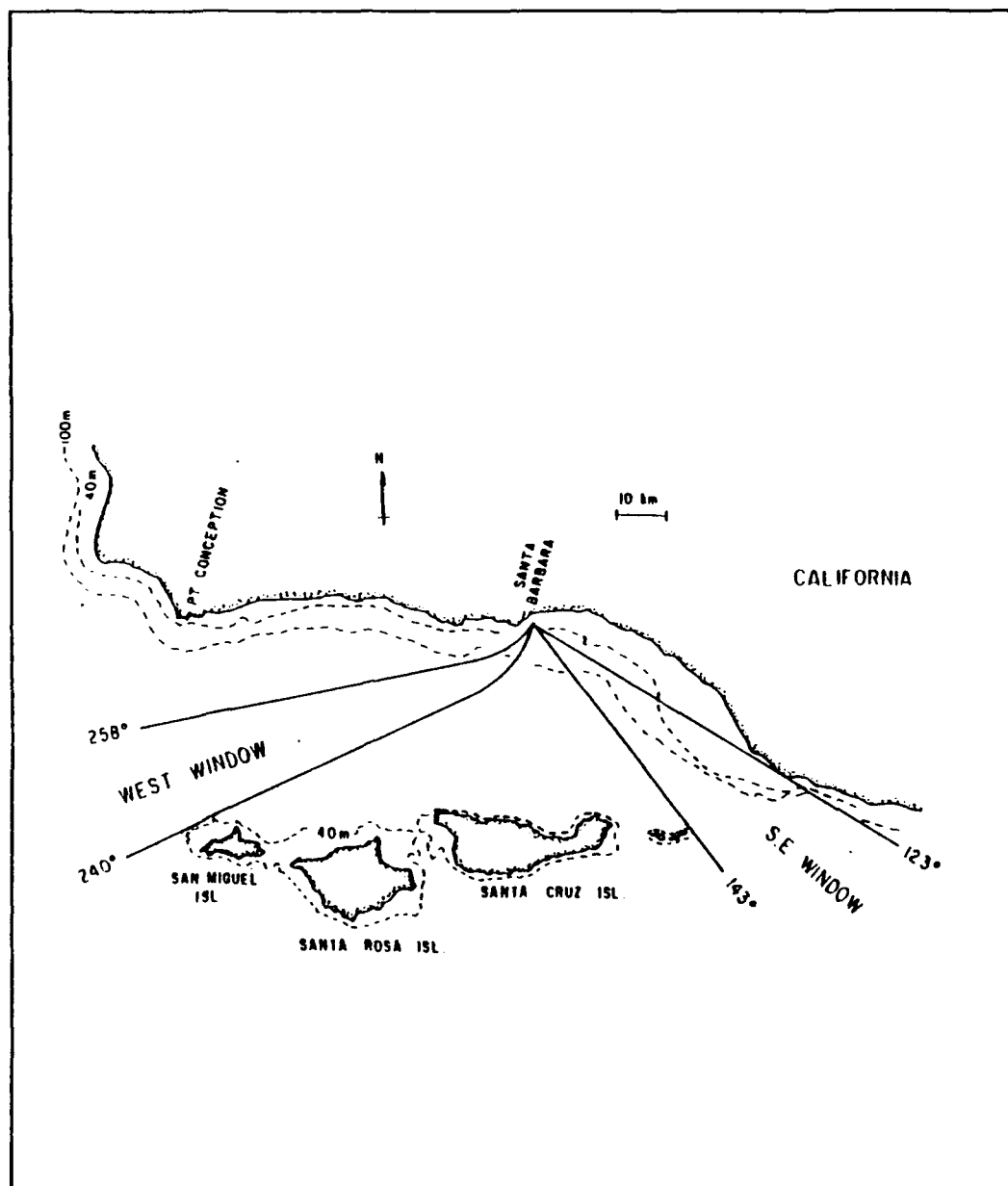


Figure 2. Windows of significant fetch at Leadbetter Beach, Santa Barbara (after Oltman-Shay and Guza, 1984).

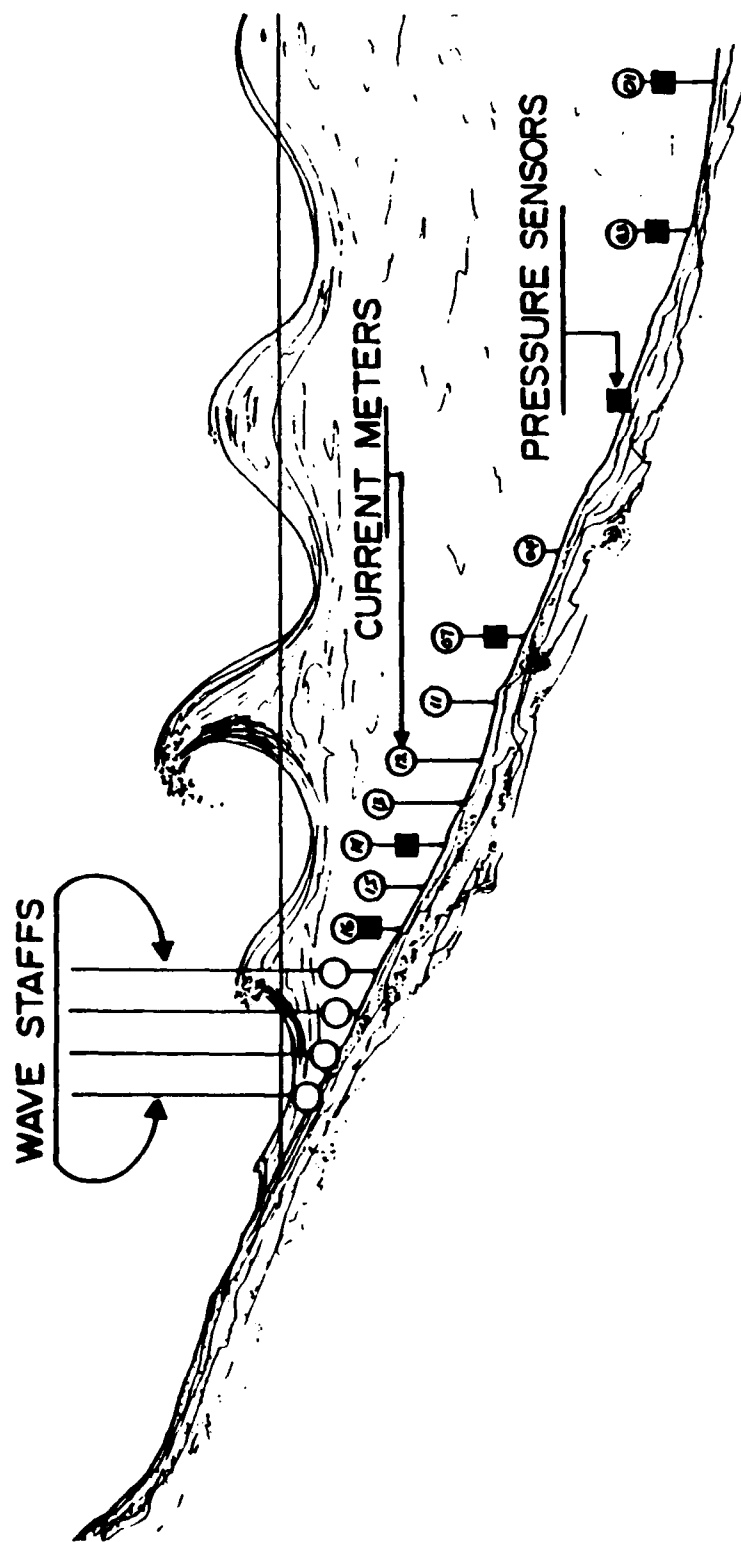


Figure 3. Cross-shore array of current meters identified by number, pressure sensors, and wave staffs, showing instrument spacing and elevations relative to a 14 second deep ocean swell wave.

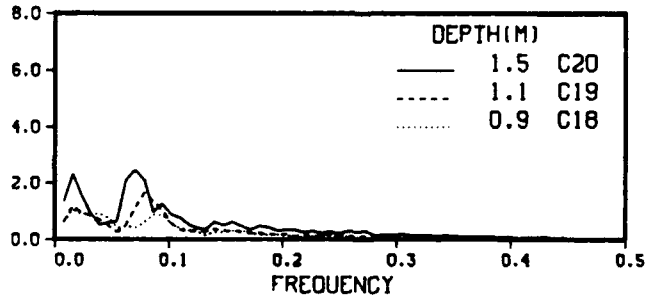
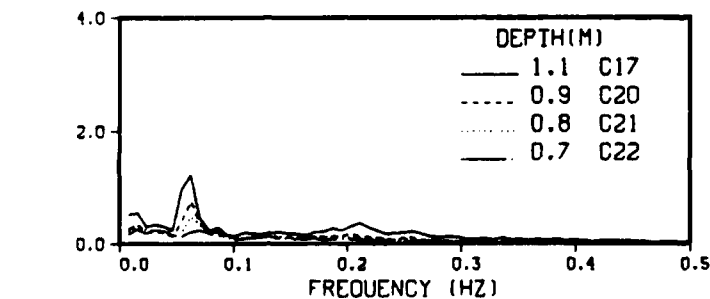
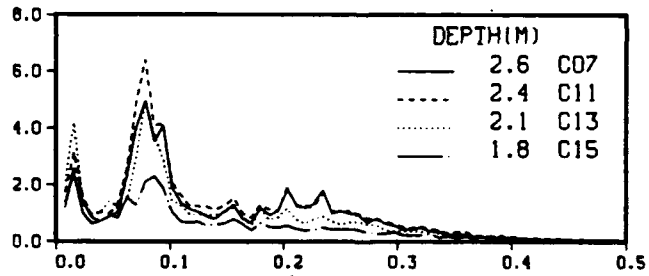
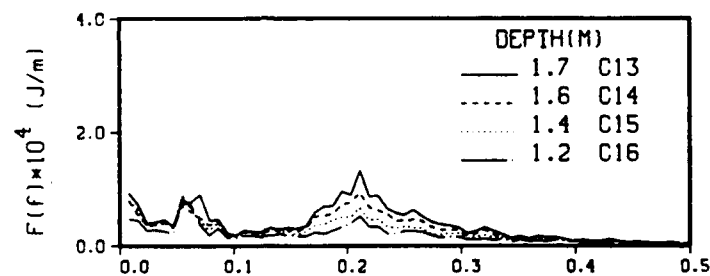
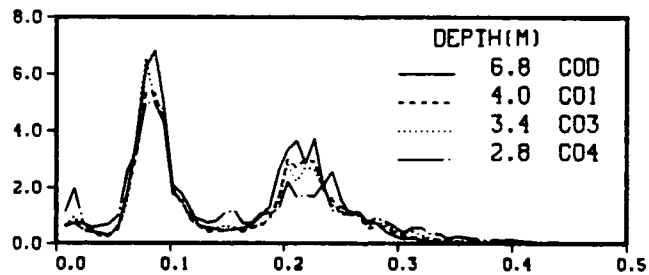
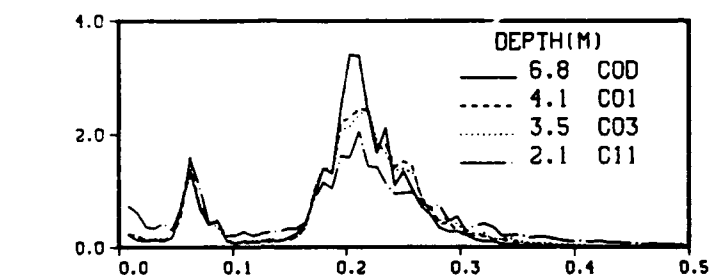
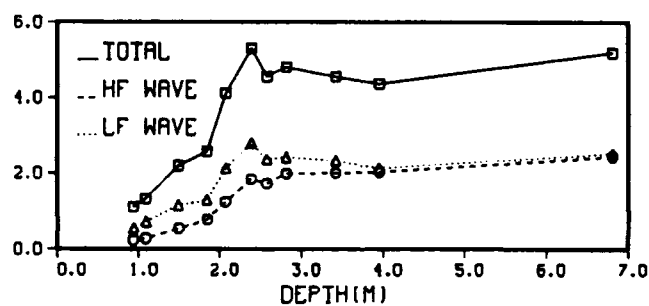
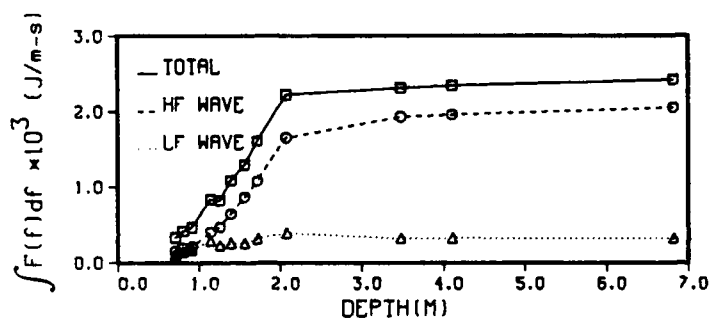


FIG. 4a. Upper panel: energy flux (LF .05-.11 Hz, HF .11-.30 Hz, total .05-.30 Hz). Lower three panels: energy flux spectra, 13 February.

FIG. 4b. Upper panel: energy flux (LF .05-.15 Hz, HF .15-.30 Hz, total .05-.30 Hz). Lower three panels: energy flux spectra, 16 February.

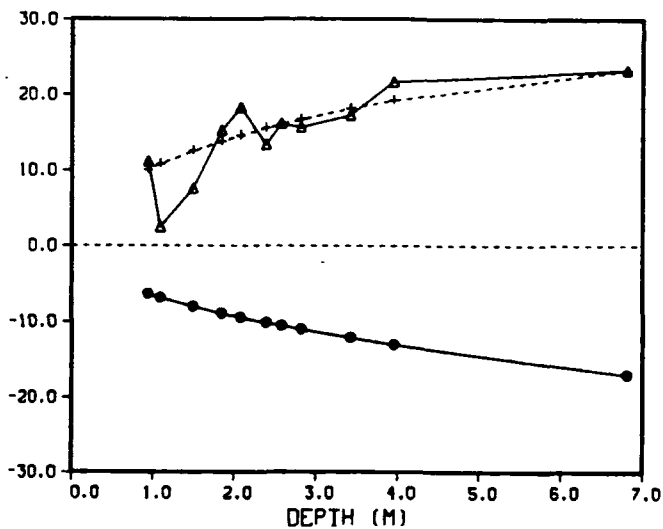
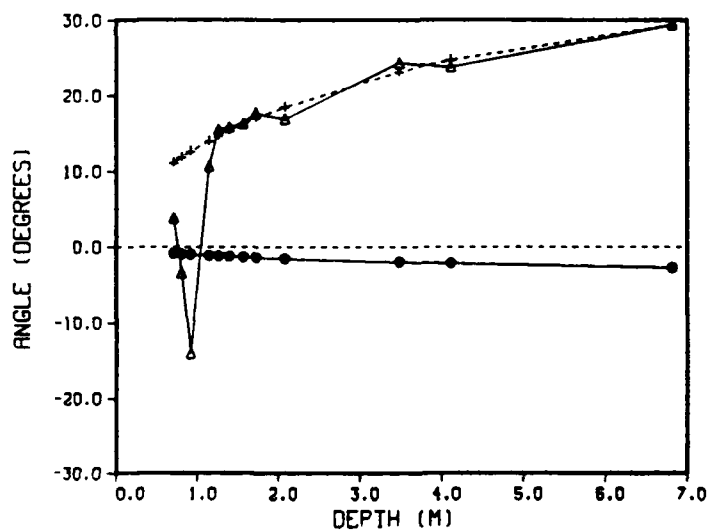
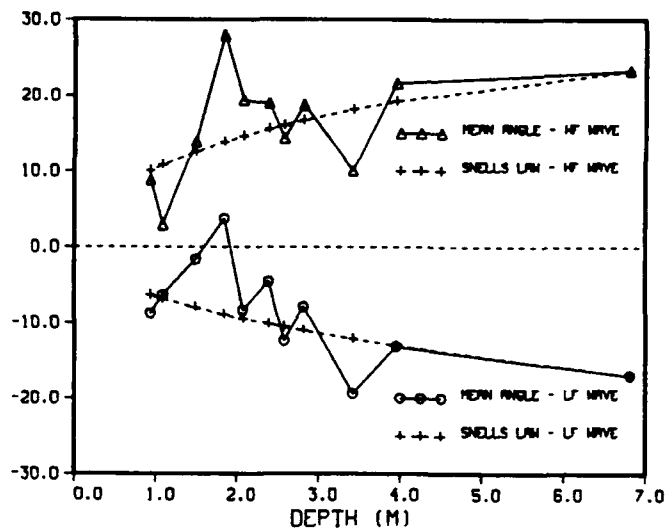
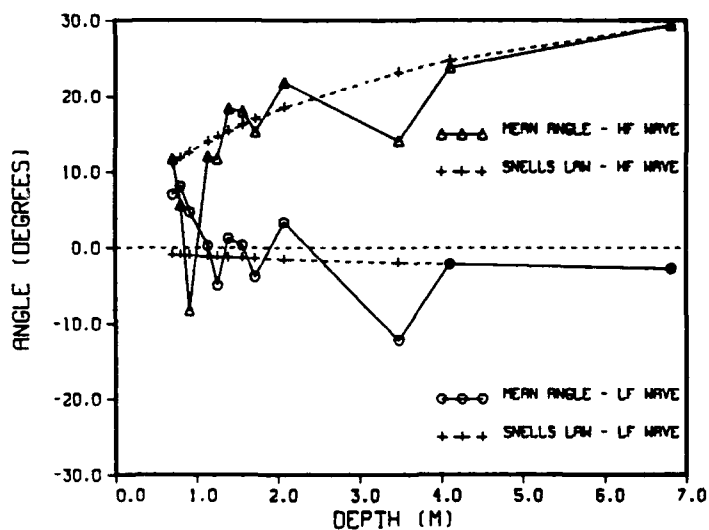


FIG. 5a. Upper panel: Measured mean wave directions (solid), predicted directions derived from Snell's Law (dashed), prior to meter rotation. Lower panel: after rotation, 13 February.

FIG. 5b. Same as Figure 5a but for 16 February.

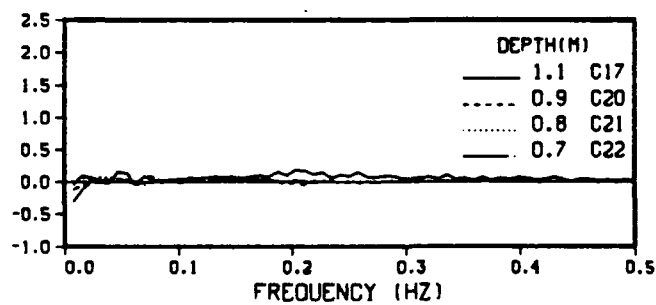
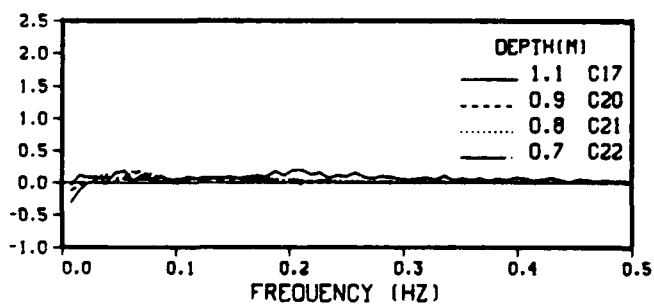
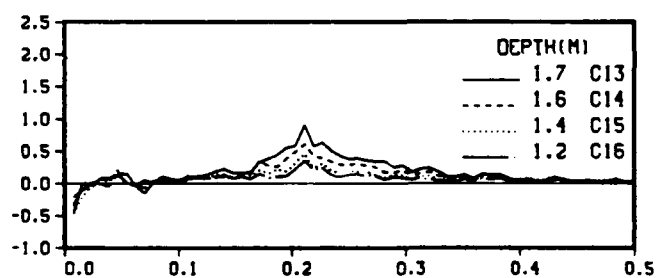
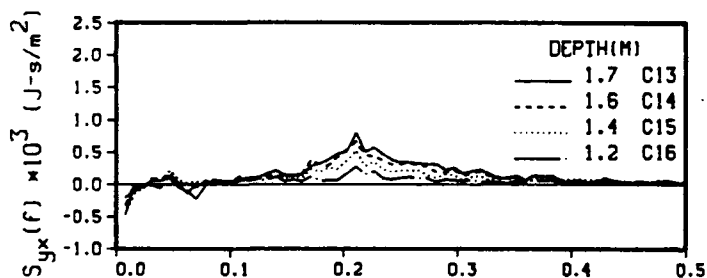
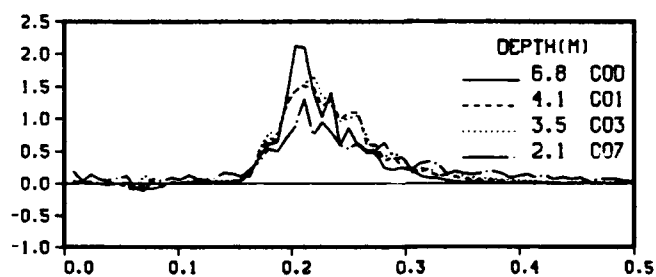
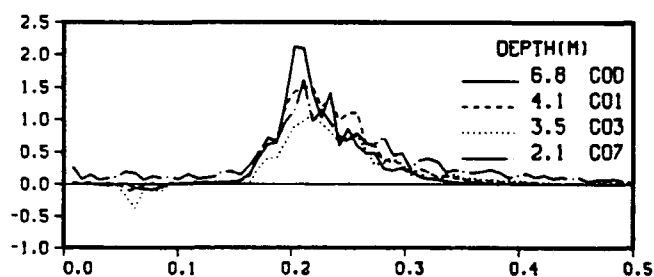
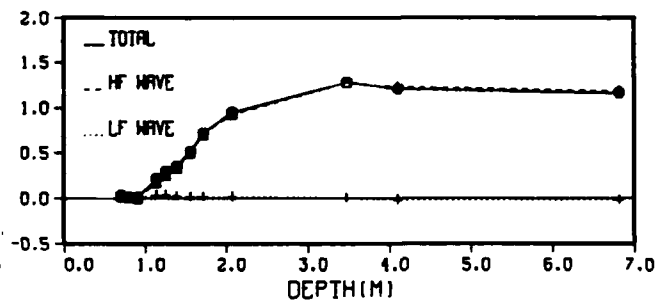
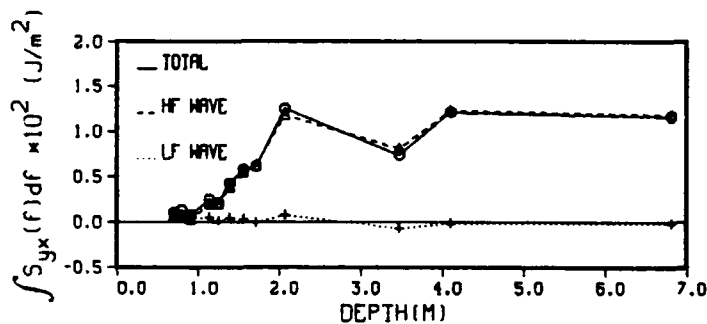


FIG. 6a. Upper panel: Radiation stress (LF .05-.11 Hz, HF .11-.30 Hz, total .05-.3 Hz). Lower three panels: radiation stress spectra. Prior to meter re-orientation, 13 February.

FIG. 6b. Same as Figure 6a but following meter re-orientation.

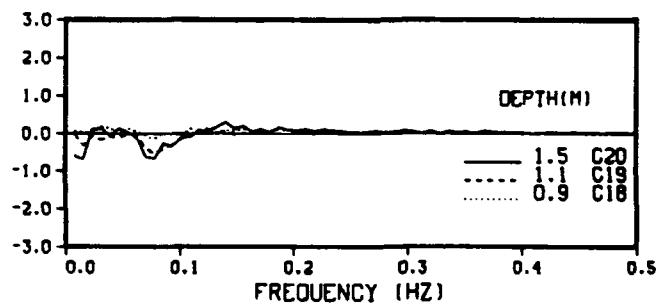
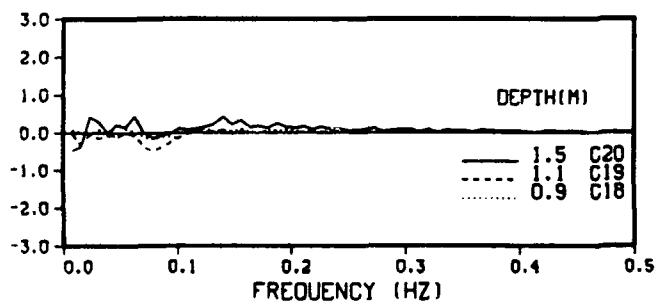
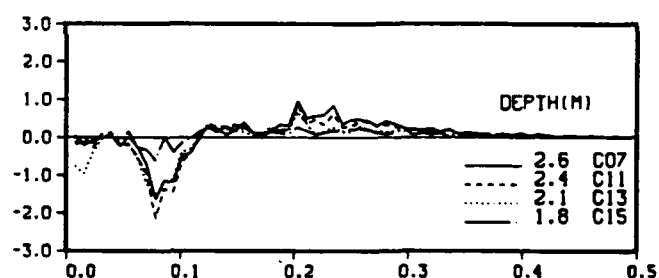
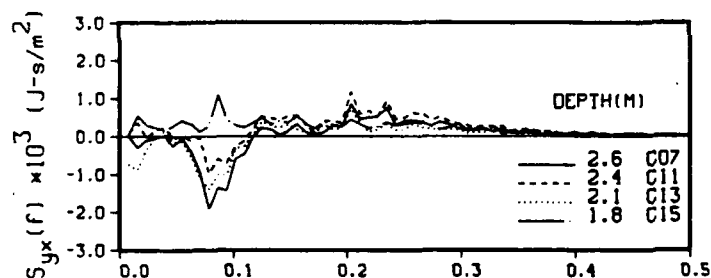
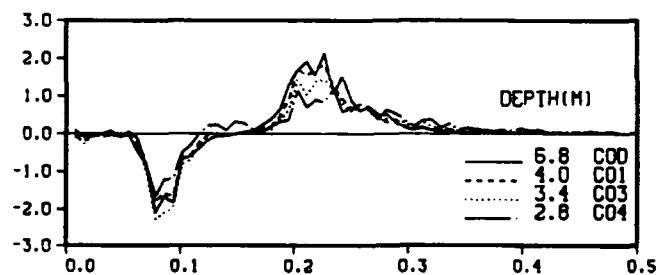
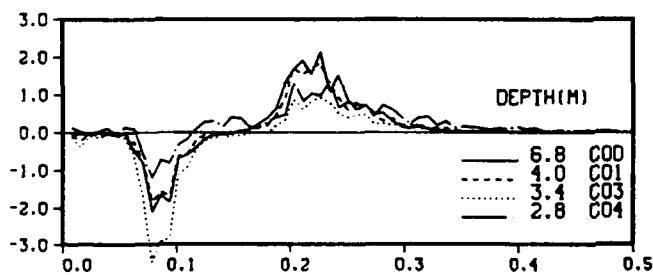
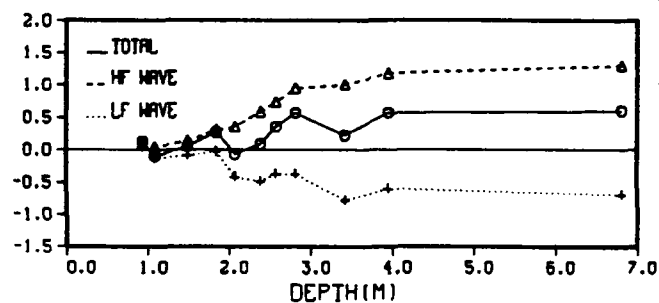
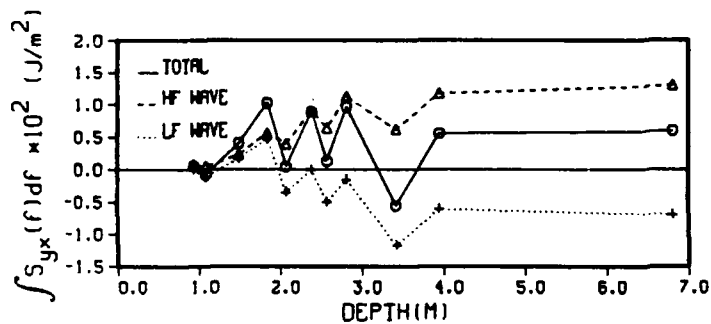


FIG. 7a. Upper panel: Radiation stress (LF .05-.15 Hz, HF .15-.30 Hz, total .05-.3 Hz). Lower three panels: radiation stress spectra. Prior to meter re-orientation, 16 February.

FIG. 7b. Same as Figure 7a but following meter re-orientation.

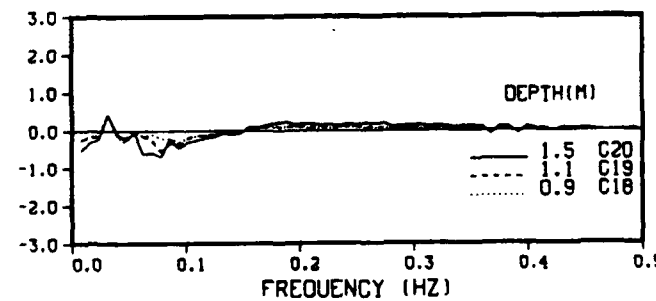
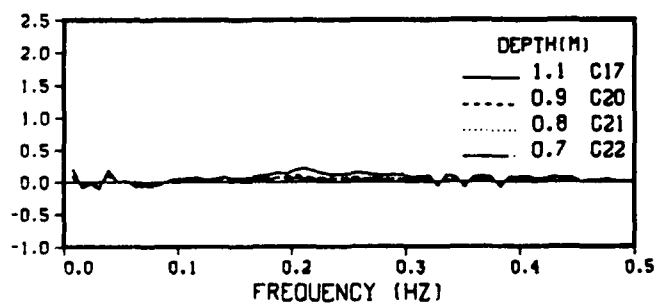
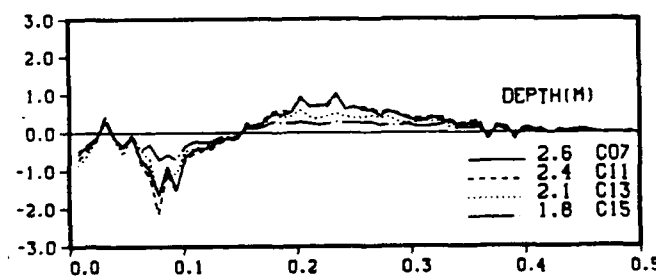
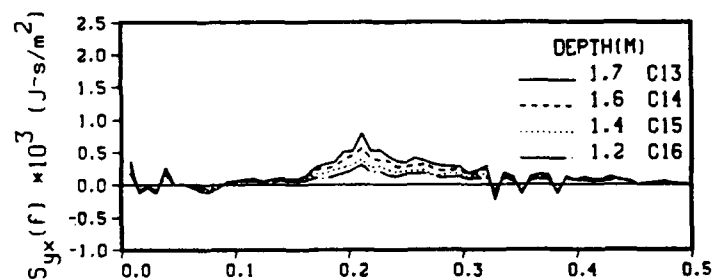
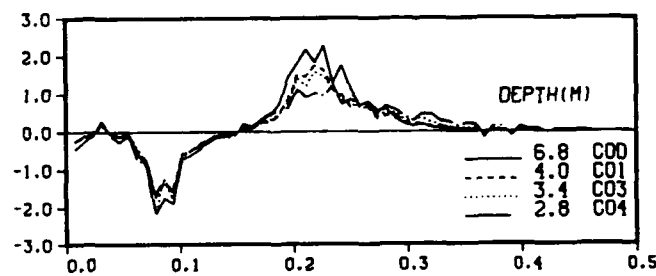
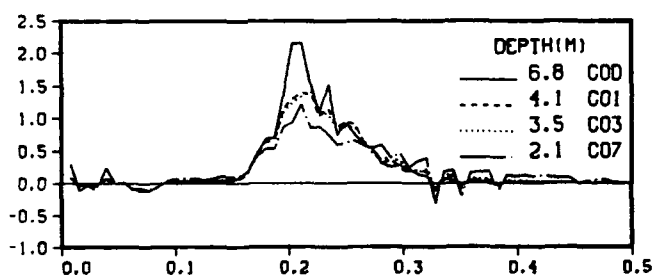
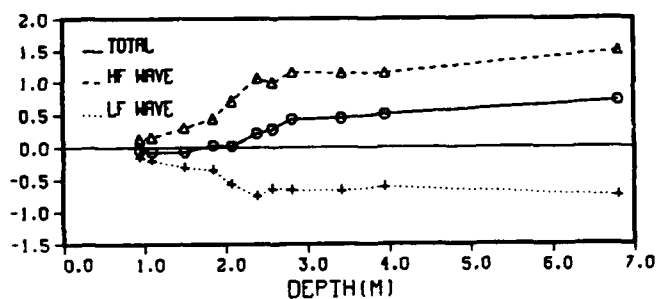
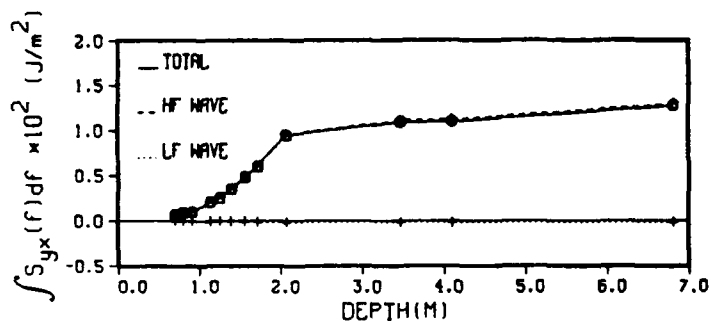


FIG. 8a. Upper panel: Radiation stress (LF .05-.11 Hz, HF .11-.30 Hz, total .05-.3 Hz). Lower three panels: radiation stress spectra. Using Eq.(3) and linear shoaling theory for mean wave directions, 13 February.

FIG. 8b. Upper panel: Radiation stress (LF .05-.15 Hz, HF .15-.30 Hz, total .05-.3 Hz). Lower three panels: radiation stress spectra. Using Eq.(3) and linear shoaling theory for mean wave directions, 16 February.

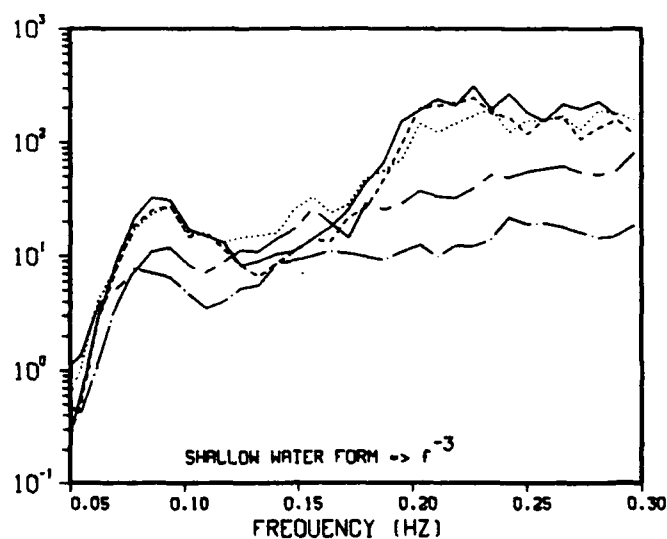
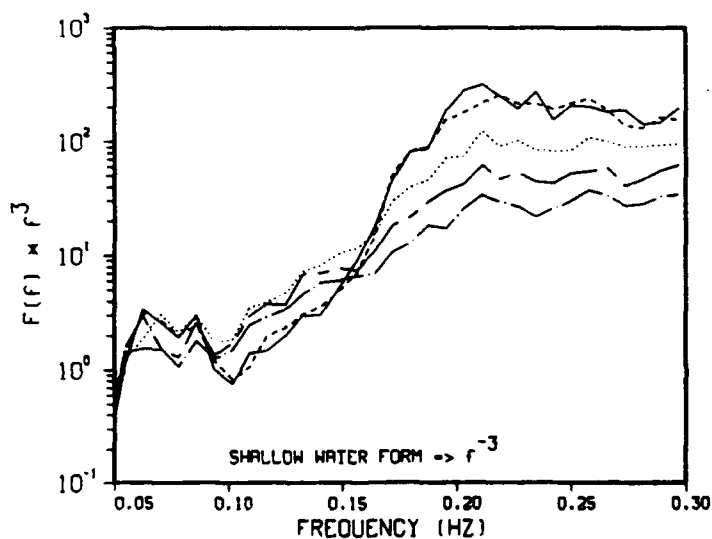
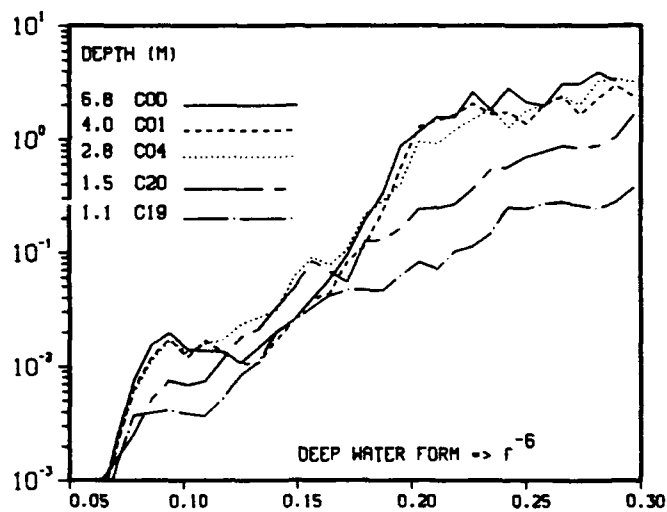
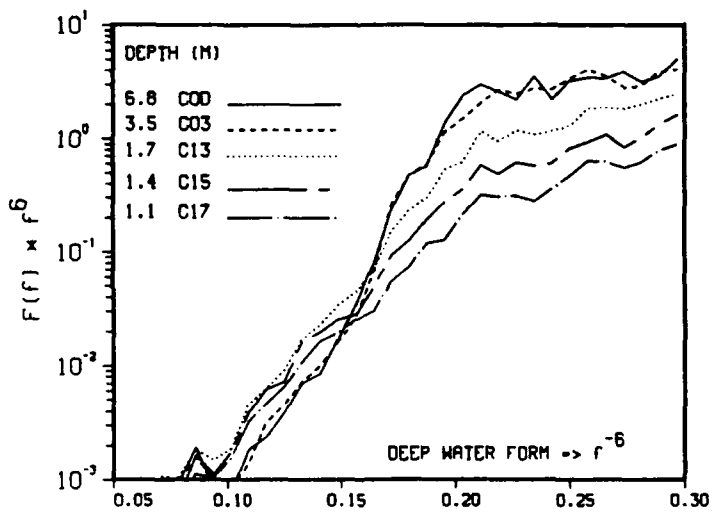


FIG. 9a. Energy flux spectra $F(f) * f^N$, upper panel: deep water form, lower panel: shallow water form, 13 February.

FIG. 9b. Same as Fig. 9a. but for 16 February.

ACKNOWLEDGEMENTS

This work was sponsored by the Naval Postgraduate School and the Office of Naval Research, Coastal Sciences Grant N00014-92-AF-00002.

LIST OF REFERENCES

- Bouws, E., H. Gunther, W. Rosenthal, and C.L. Vincent, 1985: Similarity of the wind wave spectrum in finite depth water. *J. Geophys. Res.*, **90**(C1), 975-986
- Bowen, A.J., 1969: The generation of longshore currents on a plane beach. *J. Mar. Res.*, **27**, 206-215.
- Gable, C.G., Ed., 1981: Report on data from the Nearshore Sediment Transport Study experiment on Leadbetter Beach, Santa Barbara, California, January-February 1980. IMR Ref. 80-5, Institute of Marine Resources, University of California.
- Grosskopf, W.G., D.G. Aubrey, M.G. Mattie, and M. Mathiesen, 1983: Field intercomparison of nearshore directional wave sensors. *IEEE J. Oceanic Eng.*, **OE-8**(4), 254-271.
- Guza, R.T., and E.B. Thornton, 1978: Variability of longshore currents. *Proc. 16th Int. Coastal Engineering Conf.*, New York, Amer. Soc. Civil Eng., 756-775.
- , N. Christensen, and E.B. Thornton, 1986: Observations of steady longshore currents in the surf zone. *J. Phys. Oceanogr.*, **16**(11), 1959-1969.
- Kitaigorodskii, S.A., V.P. Krasitskii, and M.M. Zaslavskii, 1975: On Phillips theory of equilibrium range in the spectra of wind generated gravity waves. *J. Phys. Oceanogr.*, **5**, 410-420.
- Long, R.B., 1980: The statistical evaluation of directional spectrum estimates derived from pitch/rollbuoy data. *J. Phys. Oceanogr.*, **10**, 944-952.
- Longuet-Higgins, M.S., 1970: Longshore currents generated by obliquely incident sea waves. *J. Geophys. Res.*, **75**, 6778-6801.
- Oltman-Shay, J., and R.T. Guza, 1984: A data-adaptive ocean wave directional-spectrum for pitch and roll type measurements. *J. Phys. Oceanogr.*, **14**, 1800-1810.
- Phillips, O.M., 1958: The equilibrium range in the spectrum of wind generated ocean waves. *J. Fluid Mech.*, **4**, 426-434.

- Smith, J.M., and C. L. Vincent, 1992: Shoaling and decay of two wave trains on a beach. Submitted for publication.
- Thompson, E.F., 1980: Energy spectra in shallow U.S. coastal waters. *Technical paper*, No. 80-2, Coastal Engineering Research Center, U.S. Army Corps of Engineers, Ft. Belvoir, Va.
- Thornton, E.B., 1970: Variations of longshore currents across the surf zone. *Proc. 12th Conf. on Coastal Engineering*, Washington, DC, ASCE, 291-308.
- , 1977: Rederivation of the saturation range in the frequency spectrum of wind generated gravity waves. *J. Phys. Oceanogr.*, 7, 137-140.
- , and R. T. Guza, 1982: Energy saturation and phase speeds measured on a natural beach. *J. Geophys. Res.*, 87(C12), 9499-9508.
- , and -----, 1983: Transformation of wave height distribution. *J. Geophys. Res.*, 88(c10), 5925-5938.
- , and -----, 1986: Surf zone longshore currents and random waves: Field data and models. *J. Phys. Oceanogr.*, 16(7), 1165-1178.

INITIAL DISTRIBUTION LIST

	No. Copies
1. Defense Technical Information Center Cameron Station Alexandria, VA 22304-6145	2
2. Library, Code 52 Naval Postgraduate School Monterey, CA, 93943-5001	2
3. Professor Edward B. Thornton, OC/Tm Department of Oceanography Naval Postgraduate School Monterey, CA 93943-5001	2
4. Professor KIM, Chang-Shik, OC/Ki Department of Oceanography Naval Postgraduate School Monterey, CA 93943-5001	1
5. Thomas D. McGowan 30 South Wig Hill Chester, CT 06412	2
6. Chairman (Code OC/Co) Department of Oceanography Naval Postgraduate School Monterey, CA 93943-5001	1
7. Chairman (Code MR/Hy) Department of Meteorology Naval Postgraduate School Monterey, CA 93943-5001	1
8. Commanding Officer Naval Research Laboratory Stennis Space Center, MS 39529-5004	1

- | | | |
|-----|---|---|
| 9. | Director
Naval Research Laboratory
Monterey, CA 93943-5006 | 1 |
| 10. | Chief of Naval Research
800 N. Quincy Street
Arlington, VA 22217 | 1 |
| 11. | Office of Naval Research (Code 420)
Naval Ocean Research and Development Activity
800 N. Quincy Street
Arlington, VA 22217 | 1 |